

# Magnetic and Electrical Transport Characteristics of $\text{La}_{0.67}\text{Sr}_{0.33}\text{Mn}_{1-x}\text{Cu}_x\text{O}_3$ ( $x = 0.10, 0.20$ , and $0.30$ ) Nano-crystalline Perovskite Oxides

Bajrang Lal Prashant<sup>1</sup>, Savita Meena<sup>2</sup>, Pritika Jai Banshiwal<sup>3</sup>

<sup>1</sup>Department of Physics, A.R.S.D. College, University of Delhi, New Delhi, 110021  
Corresponding Author Email: [bajranglal.prashant\[at\]gmail.com](mailto:bajranglal.prashant[at]gmail.com)

<sup>2</sup>Department of Chemistry, M.S.J. Government College, Bharatpur, Rajasthan, 321001

<sup>3</sup>Department of Physics, University of Rajasthan, Jaipur, 302004

Publication Date: 30 December 2023

**Abstract:** This work, copper-substituted perovskite oxides  $\text{La}_{0.67}\text{Sr}_{0.33}\text{Mn}_{1-x}\text{Cu}_x\text{O}_3$  ( $x = 0.10, 0.20$  and  $0.30$ ) have been synthesised using the sol-gel method. For examining the effect of Cu substitution (on the Mn site) on the magnetic behaviour, DC magnetization measurements have been made in the temperature range 20 K – 300 K and under external magnetic fields up to 2.5 kOe. Resistance-temperature measurements were made using the four-probe method in the 300 K – 20 K temperature range. The three samples are disordered ferromagnetic, with increasing Cu substitution, coercivity and magnetic remanence decrease. The magnetic moment does not saturate to the measuring field of 2.5 kOe, suggesting high anisotropy attributed to the nanoparticle state. The three samples do not show metallic nature; thus, no metal-insulator (M-I) transition is seen. This is due to barriers to electrical transport in the nanoparticle samples obstructing the spin-dependent electron tunnelling across the interface. On cooling the samples from the room temperature, below a certain temperature  $T_0$ , a sudden rise in resistance shows up.  $T_0$  decreases with increasing Cu, from ~102 K in the 10 % Cu substituted sample to ~60K in the 30 % Cu substituted sample.

**Keywords:** Sol-gel method, Perovskites, Magnetization

## 1. Introduction

The class of perovskite derives its name from the basic system  $\text{CaTiO}_3$ . It is denoted by a general formula unit  $\text{ABO}_3$ , where A is a monovalent, divalent or trivalent cation represented by an alkali or rare earth element, and B is correspondingly a penta, tetra or trivalent cation of the transition metal series. The basic perovskite oxide structure, of which lanthanum manganite ( $\text{LaMnO}_3$ ) is a typical example, is cubic and an antiferromagnet.  $\text{LaMnO}_3$  is also an electrical insulator. The system has a canted anti-ferromagnetic structure and shows weak ferromagnetism [1, 15]. The perovskites containing trivalent cations, e.g.  $\text{LaMnO}_3$ , are interesting due to the presence of mixed ionic-electronic conductivity and due to the significant magnetoresistance effect, known as colossal magnetoresistance (CMR), associated with a PM-FM transition [13]. The rare earth manganite perovskite with the general formula  $\text{La}_{1-x}\text{A}_x\text{MnO}_3$  ( $\text{A} = \text{Ba}, \text{Sr}, \text{Pb}$  and  $\text{Ca}$ ) are of high scientific and technological interest due to the remarkable phenomena occurring in these systems, such as Jahn-Teller distortion, double exchange, charge ordering, spin, orbit and magnetic ordering. Versatile field of applications include magnetic field sensor [4, 5], fuel cell [6, 9], spintronics materials, magneto caloric refrigeration [7], magnetically guided drug delivery and hyperthermia.

Magnetisation and electric transport behaviour of calcium-substituted system  $\text{La}_{1-x}\text{Ca}_x\text{Cr}_y\text{Mn}_{1-y}\text{O}_3$  has also been extensively studied [2, 3, 14, 17]. In the present study, we have undertaken to examine the effect of substitution of Cu for Mn in the system  $\text{La}_{0.67}\text{Sr}_{0.33}\text{MnO}_3$  in nanoparticle state. It is to be recalled that the substitution of  $1/3^{\text{rd}}$  of La by divalent Ca, Ba or Sr is known to introduce a long-range FM order into the system. The Sr-substituted perovskite has a higher  $T_c$  (and

hence stronger FM order) than the Ca-substituted one. Reported  $T_c$  of  $\text{La}_{0.7}\text{Sr}_{0.3}\text{MnO}_3$  is 338 K [12] as against 260 K for  $\text{La}_{0.7}\text{Ca}_{0.3}\text{MnO}_3$  [10, 16]. For Ba substituted perovskite  $\text{La}_{0.7}\text{Ba}_{0.3}\text{MnO}_3$ ,  $T_c$  is almost the same as the Sr substituted one [8]. We took up to study nanoparticle samples in the series  $\text{La}_{0.67}\text{Sr}_{0.33}\text{Mn}_{1-x}\text{Cu}_x\text{O}_3$  for examining the effect of substitution of Cu in the strongest FM ordered sample, and in nanoparticle regime, and compare results with those reported for substitutions of other 3d elements, viz., Cr, Co and Ti.

Samples have been prepared for three different substitutions of Cu, using the sol-gel method. Nanoparticle samples have been studied for their magnetic behaviour and magneto-resistance using Vibrating Sample Magnetometry and measuring resistance variation with temperature.

## 2. Experimental Details

### 2.1 Sample preparation

Nano-crystalline perovskite oxide samples in the series  $\text{La}_{0.67}\text{Sr}_{0.33}\text{Mn}_{1-x}\text{Cu}_x\text{O}_3$  ( $x = 0.10, 0.20$  and  $0.30$ ) were prepared by the sol-gel method using  $\text{La}(\text{NO}_3)_3 \cdot 6\text{H}_2\text{O}$ ,  $\text{Mn}(\text{NO}_3)_2 \cdot 4\text{H}_2\text{O}$ ,  $\text{Sr}(\text{NO}_3)_2$  and  $\text{Cu}(\text{NO}_3)_2 \cdot 3\text{H}_2\text{O}$  (all of 99% ) as starting materials. The nitrates were dissolved in deionized water in separate beakers. After that, the solutions were mixed, with constant stirring, with citric acid  $\text{C}_6\text{H}_8\text{O}_7$  (chelating ligand) and ethylene glycol in the ratio of 1:1:2:2.25 (lathanum nitrate: manganese and copper nitrates in proportion: citric acid: ethylene glycol). Ammonia solution was added to the solution until the pH reached 9. The temperature of the solution was increased slowly up to 100 °C, enabling water to evaporate. After evaporation of water, the material appeared black and fluffy. The synthesized

Volume 12 Issue 12, December 2023

[www.ijsr.net](http://www.ijsr.net)

Licensed Under Creative Commons Attribution CC BY

powder was calcined at 400 °C for four hours in a furnace. The calcinated samples were converted into pellets and annealed at 750 °C for 6 hours to get the desired nanoparticles.

## 2.2 Magnetization and Electric transport measurements

For studying the magnetic behaviour of the samples, magnetization measurements, such as temperature and field-dependent magnetization, have been performed on a Lakeshore Company, USA, make Vibrating Sample Magnetometer (VSM) model 7400 series at the Department of Physics, University of Rajasthan, Jaipur. These measurements have been done in the 20 K < T < 300 K temperature range and under fields up to 1 T. A closed-cycle helium refrigerator cryostat (JANIS Serial No. 17457, Janis Research Company, CCR) and electromagnet (model 643

electromagnet power supply, make company Lake Shore) have been used. The three samples' resistance measurements have been made as a function of temperature and resistance in the range 20 K < T < 300 K at NPL, New Delhi. The four-probe method was used for the measurements. For this purpose, pellets were sintered at ~100 °C. Contacts were made using silver paint, and the pellets were fixed to the sample holder using double-sided tape.

## 3. Results and Discussion

### 3.1 Magnetic behaviour

Figures 1-3 show magnetic moment versus external magnetic field (M–H) curves for the copper-substituted nanocrystalline perovskite oxide samples  $\text{La}_{0.67}\text{Sr}_{0.33}\text{Mn}_{1-x}\text{Cu}_x\text{O}_3$  (for x = 0.10, 0.20 and 0.30 ) recorded at 300 K and 20 K.

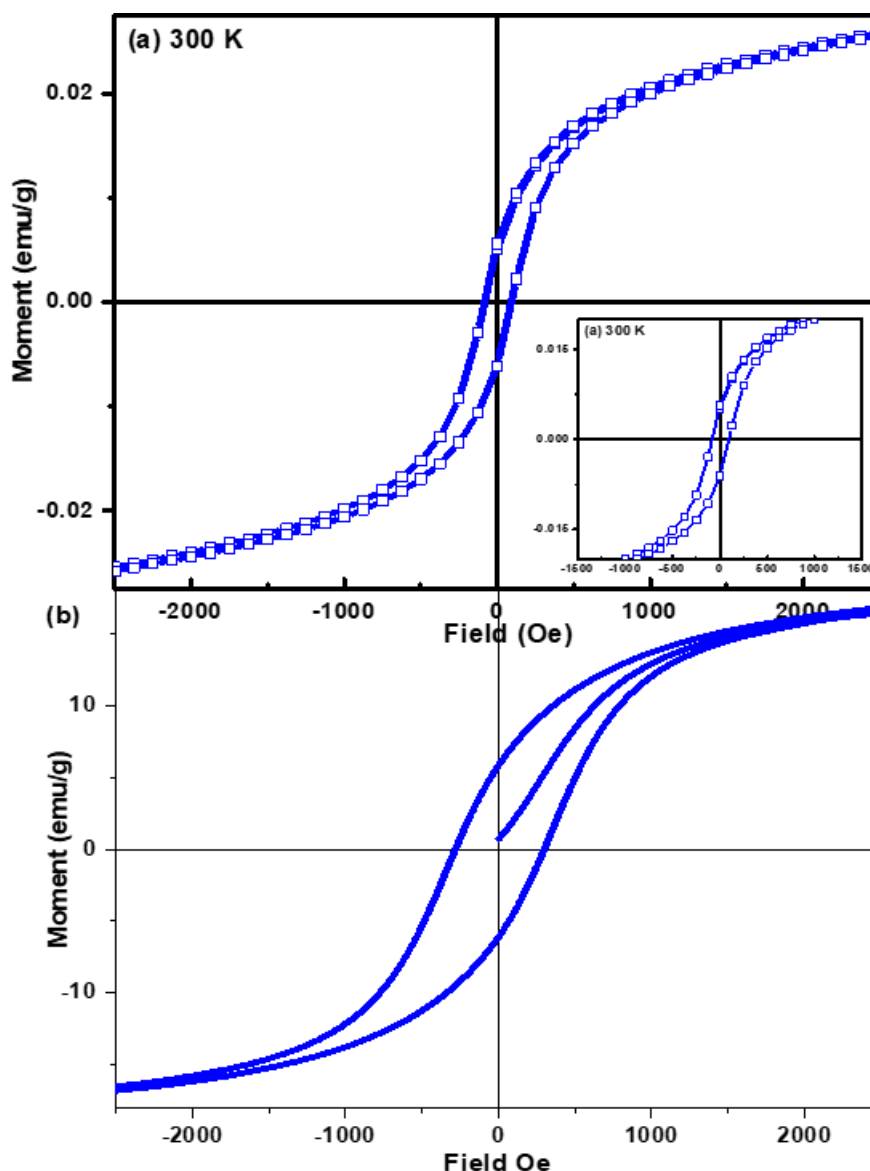


**Figure 1:** M-H curves recorded for  $\text{La}_{0.67}\text{Sr}_{0.33}\text{Mn}_{0.90}\text{Cu}_{0.10}\text{O}_3$  at (a) 300 K and (b) 20 K.

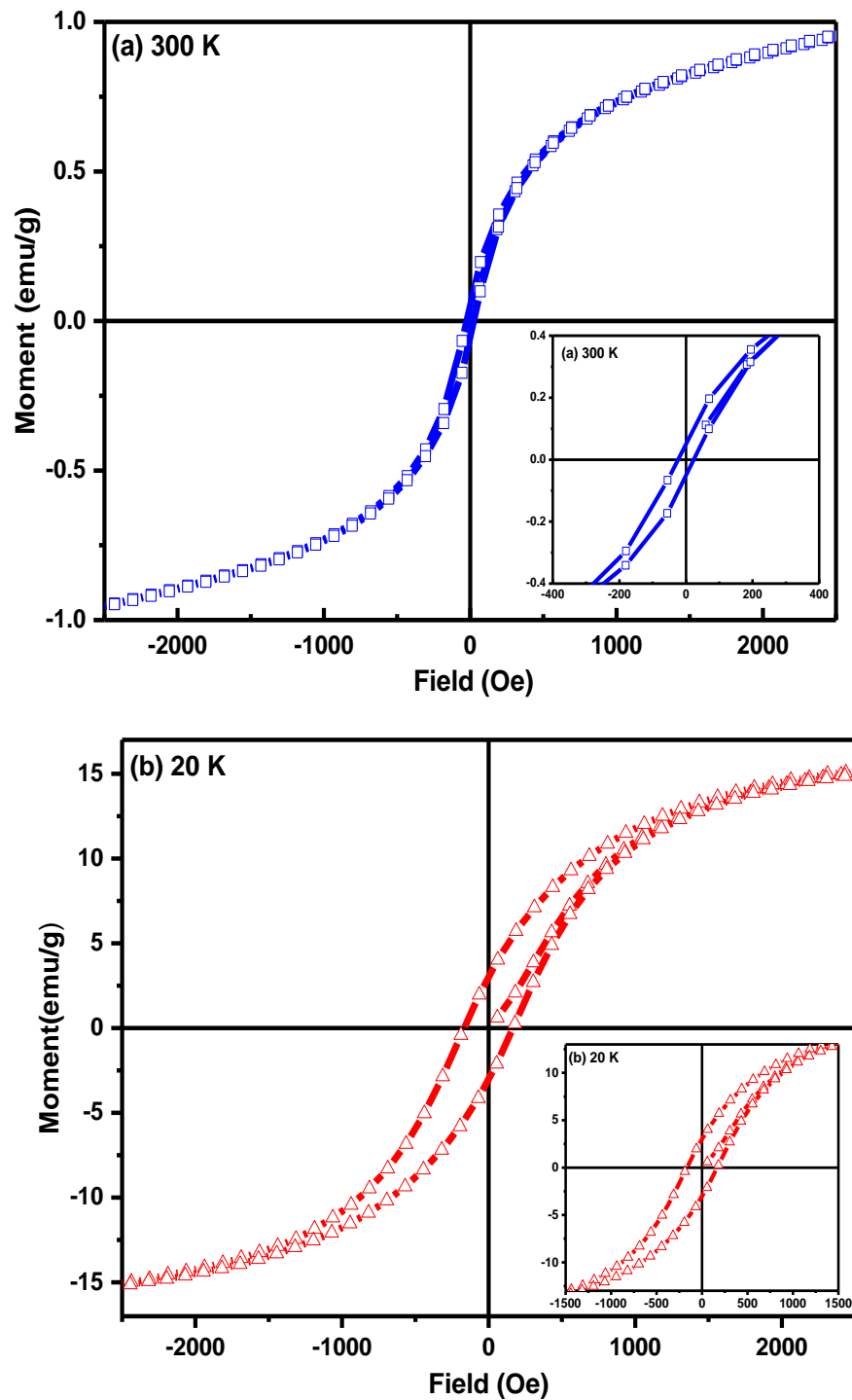
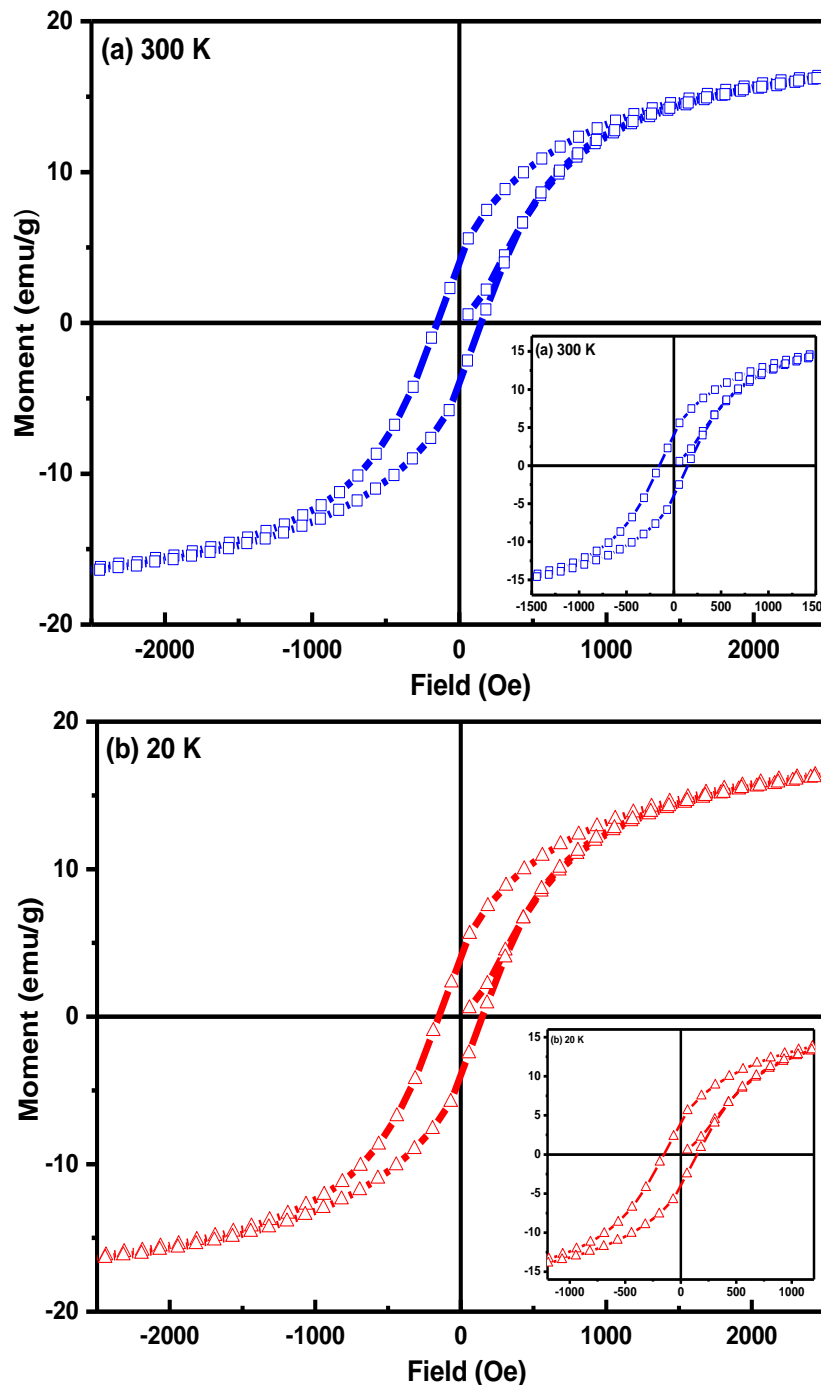


Figure 2: M-H curves recorded  $\text{La}_{0.67}\text{Sr}_{0.33}\text{Mn}_{0.80}\text{Cu}_{0.20}\text{O}_3$  at (a) 300 K and (b) 20 K.



**Figure 3:** M-H curves recorded for  $\text{La}_{0.67}\text{Sr}_{0.33}\text{Mn}_{0.70}\text{Cu}_{0.30}\text{O}_3$  at (a) 300 K and (b) 20 K.

The M–H curves clearly show that all three samples are ferromagnetic at 20K and also at 300 K. The values of  $H_c$  (coercivity),  $M_r$  (retentivity) and  $M_s$  (saturation moment – the value under 2.5 kOe) are noted in Table 1.

**Table 1:** Coercivity ( $H_c$ ), retentivity ( $M_r$ ) and saturation moment ( $M_s$  – actually the value under 2.5 kOe) at 300K and 20 K for the samples  $\text{La}_{0.67}\text{Sr}_{0.33}\text{Mn}_{0.70}\text{Cu}_{0.30}\text{O}_3$  for  $x = 0.10, 0.20$  and  $0.30$

Samples	T = 300K			T = 20K		
	$H_c$ (Oe)	$M_r$ (emu/g)	$M_s$ (emu/g)	$H_c$ (Oe)	$M_r$ (emu/g)	$M_s$ (emu/g)
$\text{La}_{0.67}\text{Sr}_{0.33}\text{Mn}_{0.90}\text{Cu}_{0.10}\text{O}_3$	~ 88	~ 0.055	0.025	~ 292	~ 6.0	16.80
$\text{La}_{0.67}\text{Sr}_{0.33}\text{Mn}_{0.80}\text{Cu}_{0.20}\text{O}_3$	~ 24	~ 0.050	0.950	~ 166	~ 3.0	15.10
$\text{La}_{0.67}\text{Sr}_{0.33}\text{Mn}_{0.90}\text{Cu}_{0.30}\text{O}_3$	~ 22	~ 0.040	0.930	~ 152	~ 4.0	16.38

Figures 1-3 show magnetization measurements, moment (emu/g) v/s temperature ( $M - T$ ), for perovskite oxides  $\text{La}_{0.67}\text{Sr}_{0.33}\text{Mn}_{1-x}\text{Cu}_x\text{O}_3$  ( $x = 0.10, 0.20$  and  $0.30$ ), recorded in zero field cooling (ZFC) and field cooling (FC) modes under external magnetic fields of (a) 100 Oe, (b) 500

Oe, and (c) 1000 Oe. These M–T curves confirm the FM nature of all three samples suggested by the M–H hysteresis measurements. Table 1 shows that as Cu concentration increases at the Mn site,  $H_c$  (coercivity) and  $M_r$  (retentivity) decrease at 300 K and 20 K. Also, M–T curves show that the

transition to the paramagnetic state is sluggish and spreads over a wide temperature range. The two observations suggest Cu is causing a weakening of the FM interaction and a localized disordered FM nature. However, the transition to the paramagnetic state is not complete till 300 K. This is a significant and surprising result. The actual paramagnetic state is not attained up to 300 K, even in a sample with 30 atomic% Cu substituted for Mn.

It is to be noted that substitution of Cr, Co or Ti is reported to cause a reduction in  $T_c$ . With the substitution of Co, the drop in  $T_c$  is about 40K per 0.05 Co [12], and with Ti substitution, it is as high as ~80K for 0.05 Ti [8]. However, it is worth noting that FM-PM transitions in these other 3d elements' substituted systems are sharp compared to the broadened ones in the Cu-substituted samples under study.

Another observation point is that for none of the three samples, at 300K and 20K, the magnetic moment shows saturation up to the measuring field of 2.5 kOe (external field). This observation conforms to localized disordered FM nature as discussed above. It is also to be noted that our samples are nano-crystalline.

Magnetic systems in nanoparticle states show high magnetic anisotropy, requiring high magnetic fields for saturation. This would also contribute to observing the non-saturating nature of the M-H curves. Nisha et al. (2013) in their study of Co-substituted  $\text{La}_{0.67}\text{Ca}_{0.33}\text{MnO}_3$  attributed their observation of

non-saturating M-H curves to the cluster glass nature of their samples [11].

### 3.2 Electrical transport behaviour

In Fig. 4, electrical resistance is plotted as a function of temperature for the three samples after they were cooled down from 300 K to ~5 K in zero field cooling mode. None of the samples show a metallic state, hence the metal-insulator (M-I) transition. On cooling the samples from room temperature, resistance increases monotonously down to a certain temperature  $T_0$  for the three samples, and below this temperature, a sudden rise in resistance is observed.

With the increasing amount of Cu, the temperature  $T_0$  decreases from ~102K in the 10% Cu-substituted sample to ~60K in the 30% Cu-substituted sample (c.f. Table 2). The complete absence of M-I transition is primarily due to the nanometric size of the particles, which incorporate a large number of grain boundaries, a reduced domain size, and a significant intergrain distance, which induce barriers to electrical transport obstructing the spin-dependent tunnelling of the electron across the interface.

It is to be noted that even for bulk particle samples, the substitution of Cr, Co and Ti causes suppression of metallic nature [8,10,11]. However, in the present study, the electrical transport behaviour largely owes to the nanoparticle nature of the samples.

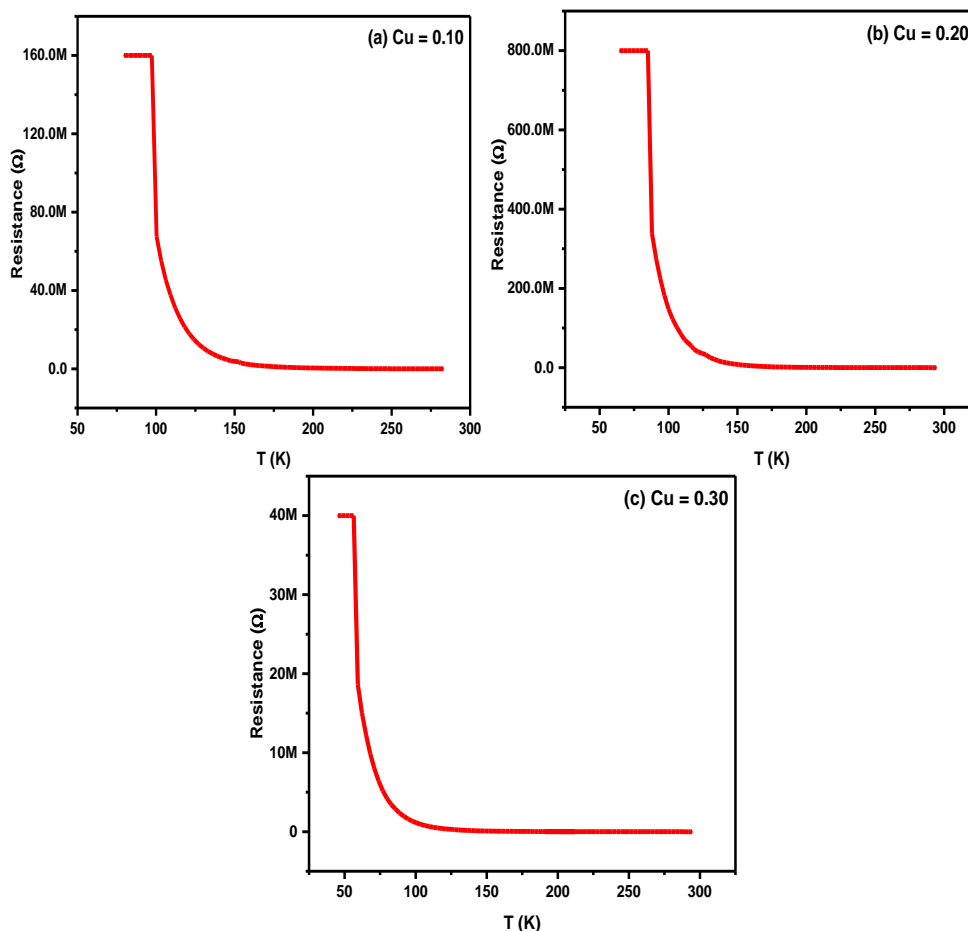


**Figure 4:** Electrical resistance as a function of temperature for the three perovskite samples  $\text{La}_{0.67}\text{Sr}_{0.33}\text{Mn}_{1-x}\text{Cu}_x\text{O}_3$  with  $x =$  (a) 0.10, (b) 0.20, and (c) 0.30 recorded following zero field cooling.

**Table 2:** Observed  $T_0$  for different levels of Cu substitution in the perovskite samples  $\text{La}_{0.67}\text{Sr}_{0.33}\text{Mn}_{1-x}\text{Cu}_x\text{O}_3$ 

S. No.	x	$T_0$ (K)
1.	0.10	102
2.	0.20	90
3.	0.30	60

#### 4. Conclusion

The three perovskite samples  $\text{La}_{0.67}\text{Sr}_{0.33}\text{Mn}_{1-x}\text{Cu}_x\text{O}_3$  (with  $x = 0.10, 0.20$  and  $0.30$ ) were prepared following the sol-gel route. M-H and M-T curves show all three samples to be ferromagnetic even at 300 K. The transition towards the paramagnetic state is sluggish and spread over a wide temperature range. With increasing amounts of Cu, coercivity and magnetic remanence decrease at room temperature and 20 K. On cooling the samples from room temperature, resistance increases monotonously to a specific temperature,  $T_0$ , followed by a sudden rise in resistance.  $T_0$  decreases with increasing Cu, from  $\sim 102$  K in the 10% Cu-substituted sample to  $\sim 60$  K in the 30% Cu-substituted sample. The absence of a metallic nature is due to barriers to electrical transport in the nanoparticle samples obstructing the spin-dependent electron tunnelling across the interface.

#### References

- [1] Wu, B. M., Li, B., Zhen, W. H., Ausloos, M., Du, Y. L., Fagnard, J. F., & Vanderbemden, P. (2005). Spin-cluster effect and lattice-deformation-induced Kondo effect, spin-glass freezing, and strong phonon scattering in  $\text{La}_{0.7}\text{Ca}_{0.3}\text{Mn}_{1-x}\text{Cr}_x\text{O}_3$ . *Journal of applied physics*, **97**(10). <https://doi.org/10.1063/1.1898438>
- [2] Cabeza, O., Long, M., Severac, C., Bari, M. A., Muirhead, C. M., Francesconi, M. G., & Greaves, C. (1999). Magnetization and resistivity in chromium doped manganites. *Journal of Physics: Condensed Matter*, **11**(12), 2569. <https://doi.org/10.1088/0953-8984/11/12/011>
- [3] Capogna L., Martinelli A., Francesconi M.G., Radaelli P.G., Carvajal J. R., Cabeza O., Ferretti M., Castellano C., Corridoni T., Pompeo N., Chang S. H., Nam H. H., Yong N. C., *Solid State Commun.* **133** (2005) 531.
- [4] Jin, S., McCormack, M., Tiefel, T. H., & Ramesh, R. (1994). Colossal magnetoresistance in La-Ca-Mn-O ferromagnetic thin films. *Journal of Applied Physics*, **76**(10), 6929-6933. <https://doi.org/10.1063/1.358119>
- [5] Balcells, L., Enrich, R., Mora, J., Calleja, A., Fontcuberta, J., & Obradors, X. (1996). Manganese perovskites: thick-film based position sensors fabrication. *Applied physics letters*, **69**(10), 1486-1488. <https://doi.org/10.1063/1.116916>
- [6] Lussier, A., Dvorak, J., Stadler, S., Holroyd, J., Liberati, M., Arenholz, E., ... & Idzerda, Y. U. (2008). Stress relaxation of  $\text{La}_{1/2}\text{Sr}_{1/2}\text{MnO}_3$  and  $\text{La}_{2/3}\text{Ca}_{1/3}\text{MnO}_3$  at solid oxide fuel cell interfaces. *Thin Solid Films*, **516**(6), 880-884. <https://doi.org/10.1016/j.tsf.2007.04.049>
- [7] Phan, M. H., Peng, H. X., Yu, S. C., Tho, N. D., Nhat, H. N., & Chau, N. (2007). Manganese perovskites for room temperature magnetic refrigeration applications. *Journal of Magnetism and Magnetic Materials*, **316**(2), e562-e565. <https://doi.org/10.1016/j.jmmm.2007.03.021>
- [8] Oumezzine, M., Peña, O., Kallel, S., Kallel, N., Guizouarn, T., Gouttefangeas, F., & Oumezzine, M. (2014). Electrical and magnetic properties of  $\text{La}_{0.67}\text{Ba}_{0.33}\text{Mn}_{1-x}(\text{Me})_x\text{O}_3$  perovskite manganites: case of manganese substituted by trivalent ( $\text{Me} = \text{Cr}$ ) and tetravalent ( $\text{Me} = \text{Ti}$ ) elements. *Applied Physics A*, **114**(3), 819-828. <https://doi.org/10.1007/s00339-013-7681-8>
- [9] Miyazaki, K., Sugimura, N., Matsuoka, K., Iriyama, Y., Abe, T., Matsuoka, M., & Ogumi, Z. (2008). Perovskite-type oxides  $\text{La}_{1-x}\text{Sr}_x\text{MnO}_3$  for cathode catalysts in direct ethylene glycol alkaline fuel cells. *Journal of power sources*, **178**(2), 683-686. <https://doi.org/10.1016/j.jpowsour.2007.08.007>
- [10] Gayathri, N., Raychaudhuri, A. K., Tiwary, S. K., Gundakaram, R., Arulraj, A., & Rao, C. N. R. (1997). Electrical transport, magnetism, and magnetoresistance in ferromagnetic oxides with mixed exchange interactions: A study of the  $\text{La}_{0.7}\text{Ca}_{0.3}\text{Mn}_{1-x}\text{Co}_x\text{O}_3$  system. *Physical Review B*, **56**(3), 1345. <https://doi.org/10.1103/PhysRevB.56.1345>
- [11] Nisha, P., Pillai, S. S., Varma, M. R., & Suresh, K. G. (2013). Influence of cobalt on the structural, magnetic and magnetocaloric properties of  $\text{La}_{0.67}\text{Ca}_{0.33}\text{MnO}_3$ . *Journal of magnetism and magnetic materials*, **327**, 189-195. <https://doi.org/10.1016/j.jmmm.2012.09.029>
- [12] Zhang, P., Yang, H., Zhang, S., Ge, H., & Hua, S. (2013). Magnetic and magnetocaloric properties of perovskite  $\text{La}_{0.7}\text{Sr}_{0.3}\text{Mn}_{1-x}\text{Co}_x\text{O}_3$ . *Physica B: Condensed Matter*, **410**, 1-4. <https://doi.org/10.1016/j.physb.2012.10.022>
- [13] Ramirez, A. P. (1997). Colossal magnetoresistance. *Journal of Physics: Condensed Matter*, **9**(39), 8171. <https://doi.org/10.1088/0953-8984/9/39/005>
- [14] Rivadulla, F., López-Quintela, M. A., Hueso, L. E., Sande, P., Rivas, J., & Sanchez, R. D. (2000). Effect of Mn-site doping on the magnetotransport properties of the colossal magnetoresistance compound  $\text{La}_{2/3}\text{Ca}_{1/3}\text{Mn}_{1-x}\text{A}_x\text{O}_3$  ( $\text{A} = \text{Co}, \text{Cr}; x \sim 0.1$ ). *Physical Review B*, **62**(9), 5678. <https://doi.org/10.1103/PhysRevB.62.5678>
- [15] Skumryev, V., Ott, F., Coey, J. M. D., Anane, A., Renard, J. P., Pinsard-Gaudart, L., & Revcolevschi, A. (1999). Weak ferromagnetism in  $\text{LaMnO}_3$ . *The European Physical Journal B-Condensed Matter and Complex Systems*, **11**, 401-406. <https://doi.org/10.1007/BF03219176>
- [16] Sun, Y., Tong, W., Xu, X., & Zhang, Y. (2001). Possible double-exchange interaction between manganese and chromium in  $\text{LaMn}_{1-x}\text{Cr}_x\text{O}_3$ . *Physical Review B*, **63**(17), 174438. <https://doi.org/10.1103/PhysRevB.63.174438>
- [17] Sun, Y., Xu, X., & Zhang, Y. (2000). Effects of Cr doping in  $\text{La}_{0.67}\text{Ca}_{0.33}\text{MnO}_3$ : Magnetization, resistivity, and thermopower. *Physical Review B*, **63**(5), 054404. <https://doi.org/10.1103/PhysRevB.63.054404>